American Mineralogist, Volume 64, pages 1175–1183, 1979

The stability of trolleite and the Al_2O_3–$AlPO_4$–H_2O phase diagram

JAY D. BASS

Department of Earth and Space Sciences
State University of New York at Stony Brook
Stony Brook, New York 11794

AND CHARLES B. SCLAR

Department of Geological Sciences, Lehigh University
Bethlehem, Pennsylvania 18015

Abstract

The univariant reaction $Al_4(PO_4)_3(OH)_3$ (trolleite) $\rightleftarrows$ 3 $AlPO_4$ (berlinite) + $\frac{1}{2}$ Al_2O_3 + 3/2 H_2O has been investigated at pressures between P_{H_2O} = 10.0 and 23.0 kbar using a piston–cylinder apparatus, and below P_{H_2O} = 5.0 kbar using standard cold-seal bombs. From these experimental results the third-law entropy and the Gibbs free energy of formation of trolleite were calculated to be 64.7±6 eu and −1452.55±3.5 kcal/mole, respectively. Based on experimental data including reversal reactions demonstrated in this study plus previous experimental results in the system Al_2O_3–$AlPO_4$–H_2O, a revised phase diagram for this system is presented wherein four univariant curves define an invariant point at 4.70 kbar and 542°C.

Background

The system Al_2O_3–$AlPO_4$–H_2O contains several unusual phosphate minerals that occur in a variety of geologic environments. Among these are berlinite ($AlPO_4$), variscite and metavariscite ($AlPO_4 \cdot 2H_2O$), augelite [$Al_2(PO_4)(OH)_3$], and trolleite [$Al_4(PO_4)_3(OH)_3$]. Although several occurrences of augelite in pegmatite have been reported, trolleite is relatively rare. It was first described by Blomstrand (1869) from the Westanå iron deposit in the Precambrian of southern Sweden, where it occurs as polycrystalline nodules in kyanite-bearing specularite–muscovite quartzite. A later hydro-thermal overprint at this locality resulted in the development of pyrophyllite, berlinite, and augelite. For some 75 years, trolleite was considered to be a discredited species until it was synthesized at high pressure and characterized by Sclar *et al.* (1963), who recognized the equivalence of their synthetic phase and Blomstrand's mineral and reestablished trolleite as a mineral species. Its crystal structure was determined by Moore and Araki (1974) on material from the White Mountains in California (Wise, 1977).

Exploratory experiments by Sclar *et al.* (1963) suggested that trolleite may be a highly pressure-dependent phase. Such phases are obviously important in providing *P–T* constraints on the history of their host rocks. The original experimental work on the synthesis and stability of trolleite was done on a bulk composition corresponding to that of variscite ($AlPO_4 \cdot 2H_2O$), which yields at high pressure not only trolleite but an aqueous phase containing phosphoric acid, through the reaction:

4 berlinite + 8 H_2O $\rightleftarrows$ trolleite + H_3PO_4 + 5 H_2O

However, inasmuch as the thermodynamic properties of phosphoric acid are not known in the pressure–temperature region of interest, we have attempted to redetermine the stability field of trolleite, using a bulk composition corresponding to trolleite in the presence of excess water by the reaction:

trolleite $\rightleftarrows$ 3 berlinite + $\frac{1}{2}$ corundum + 3/2 H_2O (1)

Since thermodynamic data are available for all phases on the right side of equation 1, it is also possible to determine the Gibbs free energy of formation, ΔG°_f, and third law entropy, S°, of trolleite at standard conditions (298.15K and 1 bar). Furthermore, the present study was carried out in a piston–cylinder apparatus and in cold-seal bombs, in which

0003–004X/79/1112–1175$02.00

pressure may be determined more accurately below 25 kbar than in the belt apparatus used in the previous experiments between 15 and 80 kbar.

Figure 1 shows the compositional relationship of trolleite and augelite within the ternary system $AlPO_4$–Al_2O_3–H_2O. Other phases within this system such as diaspore, gibbsite, and variscite do not occur in natural assemblages with augelite and trolleite and hence are not considered further. The equilibrium curve for reaction 1 will intersect 4 other univariant curves at an invariant point:

$$\text{augelite} = \text{berlinite} + \tfrac{1}{2}\ \text{corundum} + 3/2\ H_2O \qquad (2)$$

$$\text{trolleite} = \text{augelite} + 2\ \text{berlinite}$$

$$\text{(degenerate)} \qquad (3a, b)$$

$$\text{augelite} = 1/3\ \text{trolleite} + 1/3\ \text{corundum} + H_2O \qquad (4)$$

Wise and Loh (1976) investigated reactions 2 and 3 at pressures up to 3.0 kbar in cold-seal hydrothermal vessels, and based on the resultant experimental points constructed a phase diagram for the system $AlPO_4$–Al_2O_3–H_2O. The present study extends the pressure range of direct determination of equilibria in this system to 25 kbar and provides a check on the internal consistency of the published phase diagram.

Experimental technique

Standard cold-seal vessels were used at or below pressures of 5.0 kbar, and a solid-medium piston–cylinder apparatus with a 1.27 cm bore (Boyd and England, 1960) was used at or above pressures of 10 kbar. In the cold-seal bombs, temperatures were measured with chromel–alumel thermocouples. Each pressure vessel and furnace was individually calibrated, and temperatures are believed to be accurate within 5°C. Fluid pressures were measured with Heise gauges and have an estimated uncertainty of ±20 bars. In the piston–cylinder experiments, temperatures were measured with Pt–Pt10%Rh thermocouples; pressures were calculated from the oil pressure measured with a Heise gauge, times the 64:1 areal ratio. Pressure and temperature uncertainties of the piston–cylinder runs are estimated to be 1.0 kbar and 10°C, respectively. For data reduction purposes, we consider all uncertainties to be 2σ errors of the mean, as suggested by Bird and Anderson (1973). It should be noted that no correction for frictional effects, in the piston–cylinder apparatus itself or the talc pressure cell, has been made. However, we have attempted to incorporate these uncertainties in our results by performing the experiments under both instroke and outstroke conditions, with pressure overshoots of 1.5 and 2.0 kbar at desired pressures above and below 20 kbar, respectively.

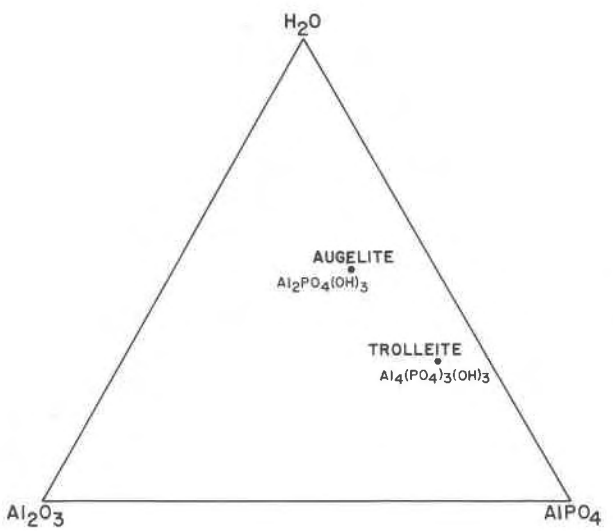

Fig. 1. Compositional ternary diagram for the system $AlPO_4$–Al_2O_3–H_2O showing the phases studied. Note that augelite, trolleite and berlinite are collinear phases.

Berlinite was prepared by heating Fisher reagent-grade hydrated aluminum phosphate ($AlPO_4 \cdot 2\ H_2O$, metavariscite) to constant weight (approximately 20 hours) at 550°C. The γ form of Al_2O_3, made by dissolving 99.999 percent pure Al wire in nitric acid and precipitating an hydroxide containing 7.70 percent H_2O by weight, was dehydrated at 1000°C and used as a source of fine-grained corundum. Trolleite and augelite were synthesized in piston–cylinder and cold-seal apparati by holding stoichiometric mixtures of berlinite, alumina, and water well within their stability fields for periods of up to 1 month. Lattice parameters for the starting materials are given in Table 1.

Sample charges for the piston–cylinder runs consisted of approximately 5–7 mg of solid and 1 mg of

Table 1. Refined unit cell parameters for starting materials

	a(A)	b(A)	c(A)	β(°)	V(A³)
Berlinite	4.947(1)	-----	10.951(3)	-----	232.13(7)
Metavariscite	8.45(1)	9.52(2)	5.17(1)	89.5(2)	415(1)
Trolleite	18.89 (1)	7.162(1)	7.142(4)	99.9(7)	951.7(7)
Augelite	13.126(5)	7.996(3)	5.075(2)	112.26(2)	492.9(4)

All data were obtained with a 114.6 mm diameter Debye-Scherrer x-ray camera using Ni filtered CuK_α radiation except for the augelite data, which were obtained with a Picker diffractometer equipped with a graphite monochrometer for the diffracted beam and CuK_α radiation. The data were reduced using the cell parameter refinement program of Appleman and Evans (1973). Numbers in parentheses are estimated standard deviations.

H_2O pressure-sealed in gold capsules. To establish reversibility of reaction at each P–T point, each run contained two charges, one consisting of the high-pressure assemblage and one the corresponding low-pressure assemblage, loaded coaxially in the sample assemblies. Pt or $Ag_{80}Pd_{20}$ capsules containing 15–20 mg of solid and 7 mg H_2O were used in the cold-seal runs, and typically two or three capsules were run simultaneously. Both the Pt and $Ag_{80}Pd_{20}$ capsules were sealed by welding. All charges were seeded with minute amounts of potential equilibrium product phases in order to minimize any metastable persistence of reactants resulting from nucleation difficulties.

After each run, the opened capsules were tested for the presence of water by placing them in a glass vial on a hot plate; condensation could then be observed at the cold end of the vial. Run products were examined by X-ray powder diffraction methods and optical microscopy. In all but a few runs, the reactions had progressed far enough for unequivocal identification of product phases, and hence the direction of reaction.

Results

The experimental results are given in Table 2 and shown graphically in Figure 2. The figure includes only the results for reaction 1, although several of the plotted points contain information pertinent to other reactions (*e.g.* runs 7b and 17b on reaction 2; run 8b on reaction 3, and run 11b on reaction 4). These latter points will be used in the next section to provide constraints on the positions of univariant lines 2 to 4 and the invariant point.

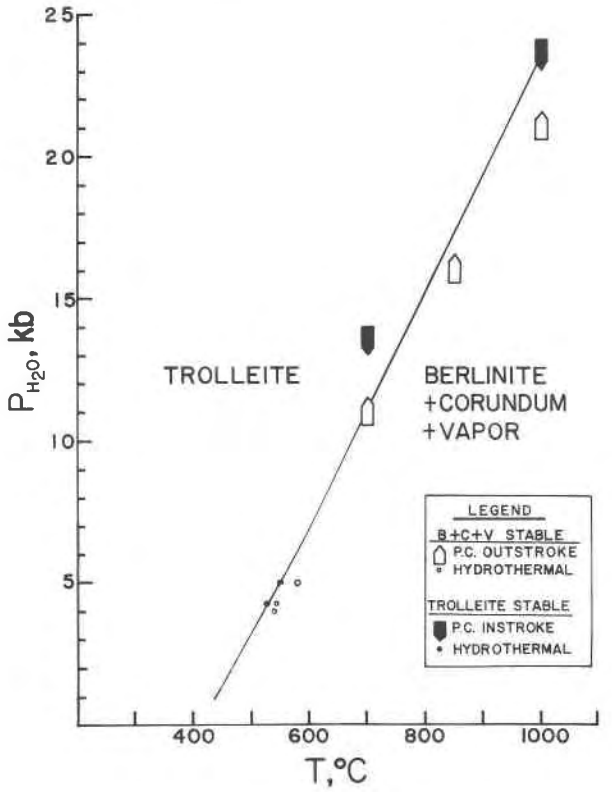

Fig. 2. Experimental results on the reaction trolleite $\rightleftarrows$3 berlinite + ½ corundum + 3/2 H_2O. The size of the symbols reflects the uncertainty in each data point. For the piston–cylinder (P.C.) runs, upward-pointing arrows indicate outstroke and downward-pointing arrows instroke conditions.

Table 2. Experimental results

Run No.	P_{H_2O}(kbar)	T(°C)	Starting Materials	Products	Time (Hours)
8b	4.00	480	A+B+(Tr)	Tr	1649
7b	4.00	540	A+(B+γ)	B+C+(X)	692
7c	4.00	540	Tr+(A+B)	B+C	692
20	4.25	530	B+C+(A+Tr)	B+C+Tr	70
17b	4.25	545	A+(B+γ+Tr)	B+X+(C)	340
17c	4.25	545	Tr+(B+A)	Tr+B+C	340
11b	5.00	550	A+(Tr+B)	Tr+C	1382
19	5.00	550	B+C+(A+Tr)	B+C+Tr	65
14b	5.00	580	Tr+(A+B)	B+C	432
25b	11.0 out	700	Tr+(B+γ)	B+C	166
44	13.5 in	700	B+C+(Tr)	B+C+Tr	18
28b	16.0 out	850	Tr+(B+γ)	B+C+Tr	89
24b	21.0 out	1000	Tr+(B+γ)	B+C+(Tr)	85
45	23.5 in	1000	B+C+(Tr)	Tr	13

Abbreviations: A, augelite; B, berlinite; C, corundum; Tr, trolleite; X, $5Al_2O_3{\cdot}H_2O$; γ, γAl_2O_3; out, outstroke; in, instroke. Starting materials in parentheses are seed crystals; product phases in parentheses are minor constituents as based on x-ray powder diffraction.

In order to bracket the reaction trolleite $\rightleftarrows$ 3 berlinite + ½ corundum + 3/2 H_2O with the piston-cylinder data, we have chosen as the most definitive bracket the dehydration of trolleite under outstroke conditions and the formation of trolleite under instroke conditions, at a given temperature. This procedure should compensate for uncertainties in pressure due to mechanical friction in the apparatus and the shear strength of the sample assembly. Although the resulting brackets are rather wide (2.5 kbar at 700°C and 1000°C), the piston–cylinder data, in conjunction with the brackets obtained from the cold-seal experiments, place very restrictive bounds on the position of the equilibrium curve for reaction 1.

Two of the cold-seal runs, 7b and 17b, yielded a fine-grained crystalline phase from the breakdown of augelite which was not present in any other run products. The X-ray powder diffraction pattern of this phase is identical with those reported by several authors (Torkar and Krishner, 1960; Aramaki and Roy, 1963; Yamaguchi *et al.*, 1964), for an aluminous material synthesized under conditions ranging from 410°C and 80 bars to 567°C and 5.2 kbar. Yamaguchi *et al.* determined the composition of this phase to be $5Al_2O_3 \cdot H_2O$. There are three possible explanations for the presence of this phase in the run products: it is a stable phase in P_{H_2O}–T region about runs 7b and 17b; it is a metastable quench product from the fluid phase; or it is a dehydration product of augelite. If the phase is stable, then it is curious that the capsules containing trolleite which were run simultaneously in the same pressure vessel (runs 7c and 17c) contained none of this phase upon quenching. Also, the ratio of $(5\ Al_2O_3 \cdot H_2O):(Al_2O_3)$ in the run products seems to decrease with longer run times, indicating that corundum is forming at the expense of $5\ Al_2O_3 \cdot H_2O$ and is more stable. Furthermore, despite a broad synthesis field, no natural occurrence of this phase has been reported. If it quenched from the fluid phase we might expect to see this phase in runs 7c and 17c, inasmuch as all of the quenched products were dominantly berlinite and corundum. Although we cannot rule out either of these possibilities with complete certainty, we suggest that this phase is a metastable breakdown product of augelite—a product that may or may not have a finite stability field.

Discussion

In order to construct the univariant curve for reaction 1, and to determine the thermodynamic properties of trolleite, the procedures outlined by Fisher and Zen (1971), and Chatterjee (1977) were followed. At a given temperature and pressure on a univariant curve the equilibrium condition is:

$$\Delta G_f^\circ(T, P) = 0 = \Delta G_{f,s}^\circ(298, 1) - \Delta S_{f,s}(298, 1)\Delta T + \Delta V_s(298, 1)\Delta P + \nu G^*_{H_2O}(T, P) \quad (5)$$

$$= \Delta H_{f,s}^\circ(298, 1) - T\Delta S_{f,s}(298,1) + \Delta V_s(298, 1)\Delta P + \nu G^*_{H_2O}(T, P) \quad (6)$$

where $G^*_{H_2O}(T, P) \equiv \Delta G_{f,H_2O}^\circ(T, 1) + G_{H_2O}(T, P) - G_{H_2O}(T, 1)$, and the other notations are as described in Appendix 1. Equations 5 and 6 are identical to equation 8 of Fisher and Zen (1971) and equation 21 of Chatterjee (1977). Both 5 and 6 assume that the difference in heat capacity between solid products and reactants in a given reaction is zero, and that the volume difference of the solid products and reactants is constant as a function of temperature and pressure. Hence, from equation 6 it is seen that a plot of $[\Delta V_s(298, 1)\Delta P + \nu G^*_{H_2O}(T, P)]$ *vs.* T should yield a straight line with a slope of $\Delta S_{f,s}(298, 1)$ and an intercept at 0K of $-\Delta H_{f,s}^\circ(298, 1)$. If $G^*_{H_2O}$ and the properties of all but one solid are known at 298K and 1 bar, $S°(298, 1)$, $\Delta H_f°(298, 1)$ and $\Delta G_f°(298, 1)$ of the unknown phase may be determined. In the following discussion, the suffix (298, 1) will be dropped, and all thermodynamic properties of solids are those at 298.15K and 1 bar unless otherwise indicated.

Using the values of $G^*_{H_2O}$ as tabulated by Fisher and Zen (1971) and calculated by Holloway (1977; personal communication), and the modified Redlich–Kwong equation of state, we have plotted $[\Delta V_s\Delta P + 3/2\ G^*_{H_2O}(T, P)]$ *vs.* T for the endpoints of our experimental brackets on reaction 1 (Fig. 3). A linear least-squares regression of the data was found to be unsatisfactory in that the resulting line did not pass through the brackets at 4.25 kbar, 5.00 kbar, and 700°C. Rather than use the least-squares line we assumed that the best fit of the data must lie within the envelope of the family of lines that pass through the brackets. Although all these lines have an equal probability of being the true equilibrium curve, we consider that line which minimizes the sum of the squares of the residuals as being most representative of the data. We found with our data that the best-fit curve which is compatible with the data set is represented by the equation:

$$(-126317 \pm 6000) + (90.01 \pm 6)\ T(\mathrm{K}) = \Delta V_s\Delta P + 3/2\ G^*_{H_2O} \quad (7)$$

The uncertainties on the parameters in equation 7 were determined by using the widest possible set of experimental brackets within the 2σ uncertainties in the data as stated above, and finding the extreme values of $\Delta S_{f,s}$ and $\Delta H_{f,s}^\circ$ that are consistent with the data. Half the difference between the extreme values is considered to be a 2σ uncertainty in each parameter. The set of temperatures and pressures at 0.5 kbar intervals which satisfy equation 7 were then found by an iterative procedure. This resulted in the equilibrium curve for reaction 1 shown in Figure 2.

Based on equation 7 and the thermodynamic data in Robie and Waldbaum (1968), the third-law entropy of trolleite at 298.15K and 1 bar, $S_{Tr}^\circ(298, 1)$, is

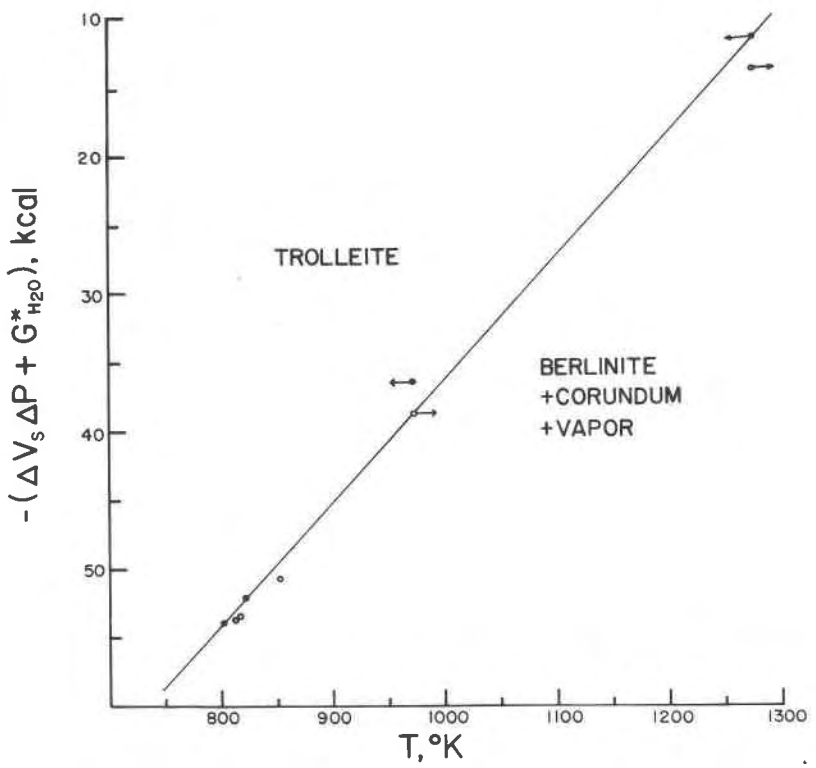

Fig. 3. A plot of T *vs.* $(\Delta V_s \Delta P + 3/2\ G^*_{H_2O})$ for reaction 1. The slope of the straight line is $\Delta S_{f,s}$ and the intercept is $-\Delta H^\circ_{f,s}$. The arrows from points representing the piston–cylinder runs at 973 and 1273K indicate how these points are affected when the experimental brackets are adjusted to accommodate the largest error on each data point. Similar displacements of the data points at lower temperatures are too small to be shown.

64.7±6 entropy units (eu), and the standard enthalpy of formation, $\Delta H^\circ_{f,Tr}$, is −1569.71±6 kcal/mol. Assigning a value of $S^\circ_{H_2O} = 10.68$ eu and a volume correction (Fyfe *et al.*, 1958, p. 27), the oxide-sum entropy of trolleite, S°_{Tr}, = 68.9 eu, which compares well with our value. The method of Fisher and Zen (1971) was applied to the narrowest experimental bracket at $P = 4.25$ kbar to calculate the Gibbs free energy of formation of trolleite. This method yields a smaller 2σ error on $\Delta G^\circ_{f,Tr}$ than that obtained by using the fitted parameters from equation 7 and the thermodynamic identity $\Delta G = \Delta H - T\Delta S$. The equilibrium line in Figure 2 indicates that at $P = 4.25$ kbar, $T_E = 531$°C. Assigning a 2σ uncertainty of ±7°C at T_E (half the bracket width) and 0.3 percent error to $G^*_{H_2O}$, $\Delta G^\circ_{f,Tr}$ is calculated to be −1452.55±3.5 kcal/mole.

In Figure 4, the equilibrium curve from Figure 2 is superimposed on the phase diagram of Wise and Loh (1976), and it is clear that the two sets of results are incompatible. Wise and Loh calculated the equilibrium curve for reaction 1 (dashed line, Fig. 4) on the basis of the experimentally-determined positions for the univariant curves of reactions 2 and 3. This dashed line is outside the indicated 2σ error bars for the position of the univariant curve for reaction 1, based on the experimental results of this study. To resolve this discrepancy, we have reevaluated their data and have found that some of their brackets about the equilibrium curves for reactions 2 and 3 are not reversed and hence do not truly define the curves. For example, they imply that reaction 2, A = B + ½ C + 3/2 H_2O, is bracketed between 506°C and 509°C at 2.0 kbar, because at 509°C augelite dehydrated and at 506°C augelite persisted. However, persistence of a phase cannot be taken as unequivocal proof of stability. The danger in such a conclusion may be demonstrated by plotting T *vs.* $\Delta V \Delta P + 3/2\ G^*_{H_2O}$ for the data of Wise and Loh on reaction 2. Using the criteria that we applied above to reaction 1, the third law entropy of augelite is −2 eu, which is physically untenable. Alternatively, using equation 5 and the procedure of Fisher and Zen (1971), the brackets indicated by Wise and Loh at 0.5

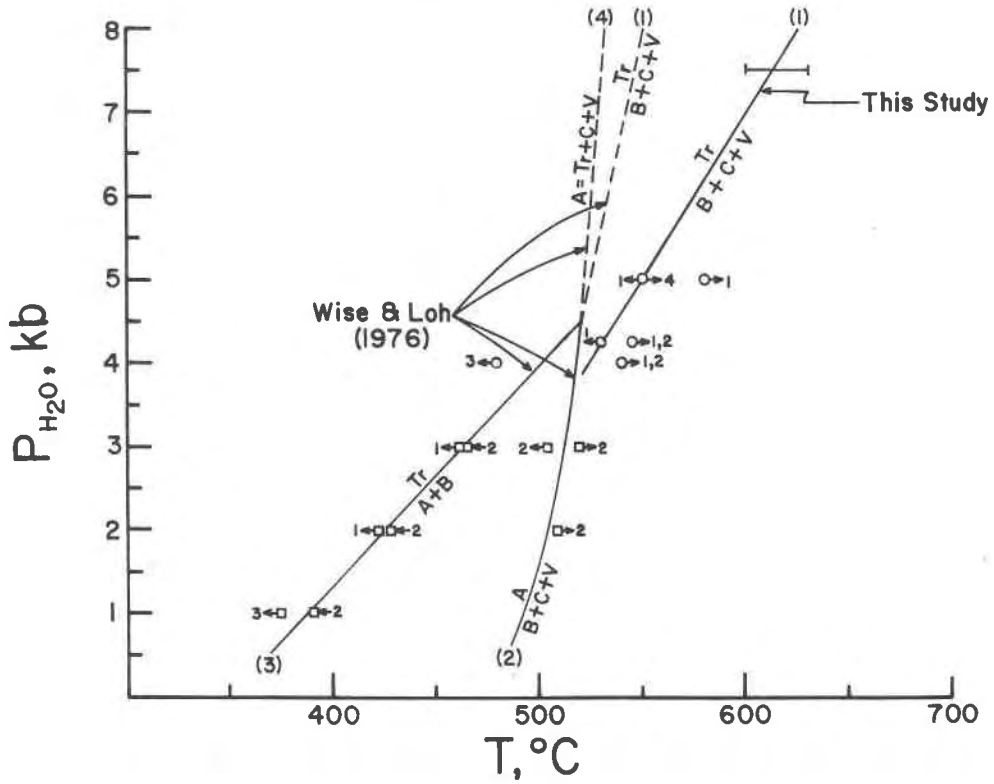

Fig. 4. The phase diagram of Wise and Loh (1976) and the univariant curve for reaction 1, Tr ⇆ 3B + ½C + V, from this study. Experimental uncertainty in the position of reaction 1 is indicated by error bars. The dashed curves for reaction 4, A = 1/3T + 1/3C + H_2O, and reaction 1 are calculated by Wise and Loh. Cold-seal bomb data from this study and Wise and Loh are indicated by circles and squares, respectively. Arrows indicate on which side of a curve a given data point must lie; the number at the end of each arrow indicates the reaction to which the data point applies.

and 3.0 kbar yield a value of S°_A = 1.4 eu. By comparison, the oxide-sum approximation of S°_A = 36 eu indicates that the data of Wise and Loh yield an unacceptably low value for S°_A.

In order to redetermine the thermochemical properties of augelite and construct a self-consistent phase diagram, we have replotted in Figure 4 only the reversed data of Wise and Loh, together with the data obtained in the cold-seal apparatus from this study.

The two brackets of Wise and Loh for reaction 2 encompass all reasonable values for the thermodynamic properties of augelite, and hence are not sufficiently restrictive for calculating both S°_A and $\Delta G^\circ_{f,A}$. This implies that a value must be assumed for either $\Delta G^\circ_{f,A}$ or S°_A in order to solve for the other quantity using equation 5. If we assume the oxide-sum entropy for augelite, S°_A, = 36±10 eu, then the midpoint of the bracket at 2.0 kbar yields a value of $\Delta G^\circ_{f,A}$ = −671.64±5 kcal/mole. The 2σ uncertainty on S°_A has been arbitrarily assigned to include all likely values, and that of $\Delta G^\circ_{f,A}$ was computed by the method of Bird and Anderson (1973). This value of $\Delta G^\circ_{f,A}$ is in agreement with $\Delta G^\circ_{f,A}$ = −671.5±1.5 reported by Wise and Loh, who assumed S°_A = 38 eu.

Several points should be noted with respect to our thermochemical calculations. First is the fact that we could have used $\Delta S^\circ_{f,s}$ and $\Delta H^\circ_{f,s}$ from equation 7 to determine $\Delta G^\circ_{f,Tr}$ and the associated 2σ uncertainty. This, however, involves the use of a parameter ($\Delta H^\circ_{f,s}$) that was determined by extrapolation over several hundreds of degrees. The extrapolation procedure magnifies any uncertainties in the data, and, in the case of our data set, resulted in a $\Delta H^\circ_{f,s}$ with a larger σ than the $\Delta G^\circ_{f,s}$ computed from the best-defined experimental bracket. If our brackets were narrower and spanned a larger temperature range, this might not have been the case. The value of $\Delta G^\circ_{f,Tr}$ determined by both methods is identical, since we have chosen an equilibrium point defined by the T *vs.* ($\Delta V_s \Delta P + \nu G^*_{H_2O}$) plot within the experimental bracket, but the uncertainty on $\Delta G^\circ_{f,Tr}$ is substantially different. We also could have determined $\Delta G^\circ_{f,Tr}$ from more than one bracket by averaging the ΔG°_f values at the bracket limits (Bird and Anderson, 1973) or by aver-

aging the ΔG_f° values of the bracket midpoints (Fisher and Zen, 1971). These methods are nearly identical and imply that, since all points within a given bracket have an equal probability of being on a univariant curve, the bracket midpoint is most representative of the information contained within the bracket. However, the wider the bracket, the larger the possible error in assuming that a bracket midpoint is an equilibrium point. Rather than calculate a number of independent free energies from brackets of varying precision, we prefer to use all of the data to define a straight line on a T *vs.* $(\Delta V_s \Delta P + \nu G^*_{H_2O})$ plot, which, in turn, defines the point within each bracket that is most likely to be on a univariant curve. Thus all the data are used to define the single best-fit values of S° and $\Delta G_{f,s}^\circ$ whose uncertainty can be computed from the tightest bracket or the T *vs.* $(\Delta V_s \Delta P + \nu G^*_{H_2O})$ plot, whichever is most restrictive. As noted by Chatterjee (1977), in the case where only one or a few brackets exist over a small temperature range, as with the reversals for reaction 2, one has little choice but to assume some reasonable estimate for S° of an unknown phase and calculate ΔG_f° and its uncertainty by the methods of Bird and Anderson (1973) and Fisher and Zen (1971).

Finally, we would like to comment on the precision of the equilibrium curve as opposed to the precision of the thermochemical data derived from it. Figure 4 shows error bars for reaction 1 which are only 30°C wide, whereas $\Delta G_{f,Tr}^\circ$ is known only within a certainty of ±3.5 kcal, which is ±90° in the position of this curve. The reason is that the difference in the thermochemical properties of reaction 1 is known better than are the properties of trolleite itself. The 2σ error estimate of $\Delta G_{f,Tr}^\circ$ reflects the uncertainties in $\Delta S_{f,s}^\circ$, the free energies of berlinite and corundum, the width of the experimental bracket at 4.25 kbar, and the uncertainty in the data points, with σ in $\Delta S_{f,s}^\circ$ the largest contributor to the total σ in $\Delta G_{f,Tr}^\circ$. However, within the range of the data the uncertainty in the position of the curve is only constrained to be intermediate between the uncertainties of the best and worst defined brackets. As a result, roundoff errors in ΔG_f° and S_f° of the unknown phases are sometimes large enough to reproduce an equilibrium curve which does not pass through all of the brackets from which the thermodynamic data were derived. To avoid this difficulty, we have reported up to four nonsignificant figures in the ΔG_f° and ΔS° values.

Figure 5 shows the equilibrium relationships of re-

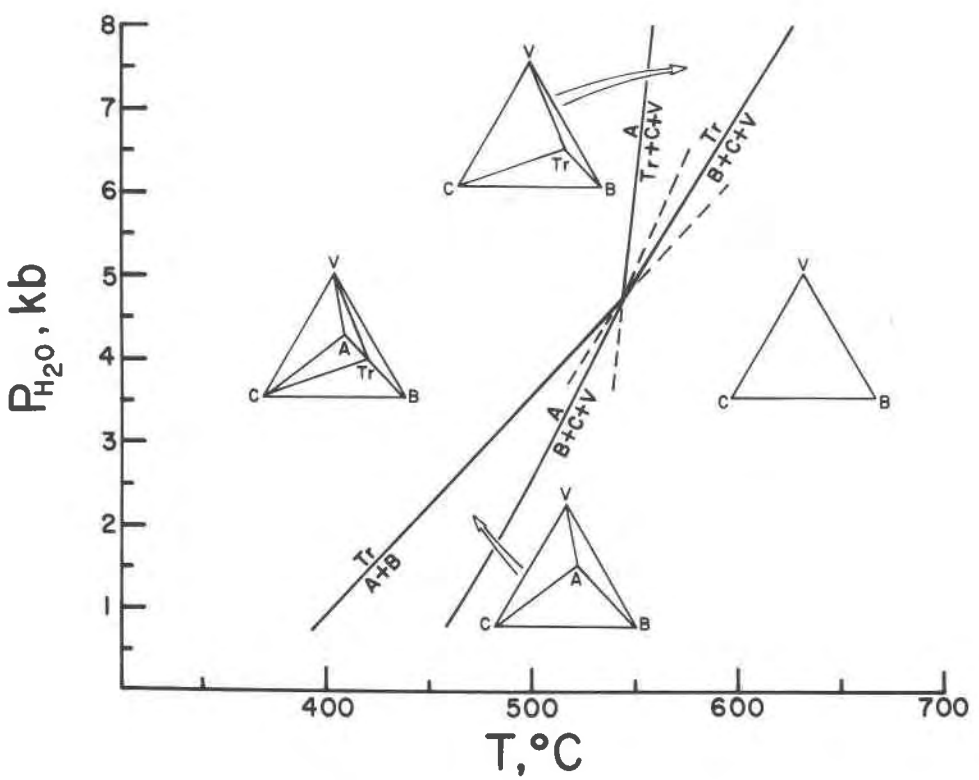

Fig. 5. Revised phase diagram for the system $AlPO_4$–Al_2O_3–H_2O about the invariant point of reactions 1–4.

actions 1 to 4 about their invariant point. The univariant curve for reaction 2 was constructed in the same way as for reaction 1, and the intersection of these two curves at 4.70 kbar and 542°C is taken as the invariant point for the four reactions. The slopes of reactions 3 and 4 at the invariant point were calculated by means of the Clapeyron equation, using the data in Robie and Waldbaum (1968) and the water data of Burnham *et al.* (1969). As a check on the internal consistency of our data and the position of the invariant point, equation 5 was solved for reactions 3 and 4, and it was found that at 4.70 kbar, both curves are within 3° of 542°C.

Note that relatively small variations in the thermochemical properties of augelite or trolleite produce significant changes in the position of the univariant curves of the phase diagram. For example, changing the entropy of augelite from 36 to 38 eu displaces the curve for reaction 4 such that the curve is on the wrong side of the only experimental point for this reaction at P_{H_2O} = 5.00 kbar and T = 550°C. Hence, we conclude that the stated uncertainties in the thermochemical properties of augelite and trolleite are rather conservative, since they do not reflect all of the restrictions imposed on ΔG_f° and S° by the data on a number of reactions. However, we have not yet developed a formalism to account simultaneously for all possible restrictions on these variables.

The largest difference between our phase diagram and that of Wise and Loh (1976) is in the position of the univariant curves for reactions 1 and 2. We conclude that Figure 5 is more realistic since it is consistent with all of the reversed data on reactions 1 to 4, whereas the diagram of Wise and Loh directly conflicts with the experimental results obtained on reaction 1 in this study. Furthermore, the equilibrium boundary for reaction 2, shown in Figure 5, is consistent with a reasonable (oxide-sum) value for the entropy of augelite, whereas the diagram of Wise and Loh requires that augelite have an unreasonably small or even negative third-law entropy. We suggest, therefore, that any geologic interpretation of occurrences of trolleite or augelite be made on the basis of the revised phase diagram.

Appendix: notation

$G_x(T, P)$; $\Delta G_{f,x}^\circ(T, P)$ Gibbs free energy of phase x at temperature T and pressure P; standard Gibbs free energy of formation of phase x from the elements at temperature T and pressure P. The standard state is 298.15K and 1 bar.

$\Delta H_{f,x}^\circ(T, P)$ Standard enthalpy of formation of phase x from the elements at temperature T and pressure P.

$S_{f,x}$; S_x° Entropy of formation of phase x from the elements; third law entropy of phase x.

E Subscript indicating equilibrium.

s Subscript indicating solid phases in a reaction.

A; B; C; Tr; V; γ Abbreviations for augelite, berlinite, corundum, trolleite, vapor phase, and γ-Al_2O_3.

ν Stoichiometric coefficient.

Acknowledgments

We thank D. H. Lindsley and H. S. Yoder, Jr. for access to experimental facilities. J. R. Holloway, T. Takahashi, and D. Eggler provided helpful comments and discussions. We are indebted to J. R. Holloway for unpublished thermodynamic data on water and to D. H. Lindsley, R. C. Liebermann, and W. S. Wise for their constructive reviews of the manuscript. The project is based in part on an M.S. thesis done at Lehigh University in the Department of Geological Sciences. The research was supported by a Sigma Xi Grant-in-Aid of Research and a GSA Penrose Bequest Grant to JDB, and by NSF grant EAR 78-02533 to D. H. Lindsley of SUNY at Stony Brook.

References

Appleman, D. E. and H. T. Evans (1973) Job 9214: Indexing and least squares refinement of powder diffraction data. *Natl. Tech. Inf. Serv., U.S. Dep. Commer., Springfield, Virginia, PB-216 188.*

Aramaki, S. and R. Roy (1963) A new polymorph of Al_2SiO_5 and further studies in the system Al_2O_3–SiO_2–H_2O. *Am. Mineral., 48,* 1322–1347.

Bird, G. W. and G. M. Anderson (1973) The free energy of formation of magnesian cordierite and phlogopite. *Am. J. Sci., 273,* 84–91.

Blomstrand, C. W. (1869) Über neue schwedische Mineralien. *Neues Jahrb. Mineral. Geol. Paleontol.,* 481–482.

Boyd, F. R. and J. L. England (1960) Apparatus for phase equilibrium measurements at pressures up to 50 kilobars and temperatures up to 1750°C. *J. Geophys. Res., 65,* 741–748.

Burnham, C. W., J. R. Holloway and N. F. Davis (1969) Thermodynamic properties of water to 1000°C and 10,000 bars. *Geol. Soc. Am. Spec. Pap. 132.*

Chatterjee, N. D. (1977) Thermodynamics of dehydration equilibria. In D. G. Fraser, Ed., *Thermodynamics in Geology,* p. 137–159. D. Reidel, Dordrecht, Holland.

Fisher, J. R. and E-an Zen (1971) Thermochemical calculations from hydrothermal phase equilibrium data and the free energy of H_2O. *Am. J. Sci., 270,* 297–314.

Fyfe, W. S., F. J. Turner and J. Verhoogen (1958) Metamorphic reactions and metamorphic facies. *Geol. Soc. Am. Mem. 73.*

Holloway, J. R. (1977) Fugacity and activity of molecular species in supercritical fluids. In D. G. Fraser, Ed., *Thermodynamics in Geology,* p. 161–182. D. Reidel, Dordrecht, Holland.

Moore, P. B. and T. Araki (1974) Trolleite, $Al_4(OH)_3(PO_4)_3$: a very dense structure with octahedral face-sharing dimers. *Am. Mineral., 59,* 974–984.

Robie, R. A. and D. R. Waldbaum (1968) Thermodynamic prop-

erties of minerals and related substances at 298.15°K (25.0°C) and one atmosphere (1.013 bars) pressure and at high temperatures. *U.S. Geol. Surv. Bull. 1259.*

Sclar, C. B., L. C. Carrison and C. M. Schwartz (1963) Synthesis and properties of trolleite (aluminian lazulite?), a high-pressure mineral from the Westanå iron deposit, Kristianstad, Sweden. *Geol. Soc. Am. Spec. Pap., 76,* 145.

Torkar, K. and H. Krischner (1960) Untersuchungen über Aluminianhydroxyde und -Oxyde, 4. *Mitt. Monatsh. Chem., 91,* 658–668.

Wise, W. S. (1977) Mineralogy of the Champion mine, White Mountains, California. *Mineral. Rec., 8,* 478–486.

——— and S. E. Loh (1976) Equilibria and origin of minerals in the system Al_2O_3–$AlPO_4$–H_2O. *Am. Mineral., 61,* 409–413.

Yamaguchi, G., H. Yanagida and S. Ono (1964) A new alumina hydrate, "tohdite" ($5Al_2O_3 \cdot H_2O$). *Bull. Chem. Soc. Japan, 37,* 752–754.

Manuscript received, March 19, 1979;
accepted for publication, June 2, 1979.